Microscopic studies on Thermosipho globiformans implicate a role of the large periplasm of Thermotogales

doi: 10.1007/s00792-012-0481-9

Microscopic studies on *Thermosipho globiformans* implicate a role of the large periplasm of Thermotogales

Tomohiko Kuwabara · Kensuke Igarashi

Graduate School of Life and Environmental Sciences, University of Tsukuba, Tsukuba, Ibaraki 305-8572, Japan

Abbreviations

ATOC	Anaerobic thermophile observation chamber
FE-SEM	Field-emission scanning electron microscopy
HTM	High-temperature microscopy
OM	Outer membrane
TEM	Transmission electron microscopy

Corresponding author

Tomohiko Kuwabara

Address: Graduate School of Life and Environmental Sciences, University of Tsukuba, Tsukuba, Ibaraki 305-8572, Japan

E-mail: kuwabara@biol.tsukuba.ac.jp

Fax: +81 29 853 6614

Abstract *Thermosipho globiformans* is a member of Thermotogales, which contains rod-shaped, Gram-negative, anaerobic (hyper)thermophiles. These bacteria are characterized by an outer sheath-like envelope, the toga, which includes the outer membrane and an amorphous layer, and forms large periplasm at the poles of each rod. The cytoplasmic membrane and its contents are called “cell,” and the toga and its contents “rod,” to distinguish between them. Optical cells were constructed to observe binary fission of *T. globiformans*. High-temperature microscopy of rods adhering to optical cell’s coverslips showed that the large periplasm forms between newly divided cells in a rod, followed by rod fission at the middle of the periplasm, which was accompanied by a sideward motion of the newly generated rod pole(s). Electron microscopic observations revealed that sessile rods grown on a glass plate have nanotubes adhered to the glass, and these may be involved in the sideward motion. Epifluorescence microscopy with a membrane-staining dye suggested that formation of the septal outer membrane is distinct from cytokinesis. Transmission electron microscopy indicated that the amorphous layer forms in the periplasm between already-divided cells. These findings suggest that the large periplasm is the structure in which the septal toga forms, an event separate from cytokinesis.

Key words Anaerobic bacteria, Cell division, Deep-sea thermophiles, Nanotubes, Toga

Introduction

The order Thermotogales is one of the deepest branching lineages in the domain Bacteria (Woese et al. 1990). The members of Thermotogales can be distinguished from other bacteria by using optical microscopy due to the presence of the large periplasm that is formed by the sheath-like envelope, i.e., the toga, in each rod (Huber and Stetter 1992). The toga includes an outer membrane (OM) and an amorphous layer with a gapped contour on the periplasmic side (Huber et al. 1986; Andrews and Patel 1996; L'Haridon et al. 2001; Wery et al. 2001; Miranda-Tello et al. 2004). Although the large periplasm has a phylogeny-symbolizing morphology, its physiological role remains unknown. In multicellular rods, cells exist in chains with each periplasm between the cells inside a sheath. While these rods are rare, they have been observed in many species of Thermotogales. Direct observation of binary fission may provide insights into the role of the large periplasm and the formation of these multicellular rods in Thermotogales.

Thermosipho globiformans is a recent addition to Thermotogales (Kuwabara et al. 2011); it forms eukaryotic-like multicellular spheroids in the early growth phases, and the cells grow very fast with a doubling time of 24 min in the mid-exponential phase. It has no flagellum and exhibits no motility. These characteristics led us to use *T. globiformans* for the direct observation of binary fission by using high-temperature microscopy (HTM).

HTM was originally developed by Gluch et al. (1995) to observe the motility and thermotactic responses of *Thermotoga maritima* (Huber et al. 1986) by using optical cells made from capillaries, both ends of which were sealed with vacuum grease. Horn et al. (1999) observed binary fission of hyperthermophilic crenarchaea by using a high-intensity dark-field microscope with capillaries,

both ends of which were sealed by melting the glass with heat. Deguchi and Tsujii (2002) also developed an HTM technique to observe the behavior of microorganisms at high pressure and temperature. However, these techniques require the use of a considerable amount of equipment, and it is unknown whether the capillary cells have sufficient resolution to distinguish the periplasm of Thermotogales (Gluch et al. 1995).

In the present study, disposable optical cells were manually constructed for the growth of anaerobic thermophiles by using a high-temperature durable glue, and these optical cells were used to directly observe the binary fission of *T. globiformans* by HTM. Results of HTM observations inspired us to conduct electron and epifluorescence microscopy to observe the rod surface and the intercellular periplasm. The results of these studies suggest that the large periplasm plays a role in the formation of multicellular rods in Thermotogales.

Materials and methods

Cultivation of *T. globiformans*

T. globiformans MN14 (Kuwabara et al. 2011) was anaerobically batch-cultured in Tc medium (Kuwabara et al. 2005) at 68°C, unless otherwise stated. In some experiments, cells were cultured at different temperatures or in Tc medium devoid of elemental sulfur (Tc–S^0 medium).

Construction and incubation of anaerobic thermophile observation chambers (ATOCs)

84 A Pyrex glass tube (outside diameter, 20 mm; glass thickness, 1.6 mm) was cut into 10-mm-long
85 pieces. These pieces were coated with dimethyl polysiloxane (Siliconize L–25; Fuji Systems,
86 Tokyo, Japan) to reduce surface tension. A Pyrex piece was affixed to the center of a coverslip (30
87 × 30 × 0.17 mm; MATSUNAMI, Kishiwada, Japan) by using a high-temperature durable glue
88 (Super X2; Cemedine, Tokyo, Japan, stated to be durable up to 120°C) and a toothpick in an
89 anaerobic workstation in which the gas phase was N_2:H_2:CO_2 = 80:10:10. The surfaces for adhesion
90 should be dry. This and the following adhesion steps were carried out in the workstation; adhesion
91 under air sometimes resulted in the leakage of ATOCs during HTM observation, which was
92 indicated by a change in the color of resazurin in the medium. The product was left overnight in the
93 workstation and weighed down using a disposable tube filled with 50 ml of water. A 0.5-ml
94 microcentrifuge tube was cut 7 mm from the top, and the lid was removed. The resulting open end
95 of the tube was used as the partition of an ATOC and was affixed to the coverslip by using the glue
96 and a toothpick, avoiding the center of the coverslip, in order to secure the light path for HTM. The
97 resultant product was an intermediate ATOC construction (Fig. 1a). The intermediate was sterilized Fig. 1
98 using a 70% (v/v) ethanol spray and dried in a clean oven.
99 Immediately before the ATOC was completed, Tc medium devoid of Na_2S was autoclaved at
100 110°C for 5 min for degassing. The medium was taken out from the autoclaving instrument when
101 the temperature decreased to 90°C. In the workstation, 2 ml of medium were supplemented with 10
102 µl of 10% $Na_2S·9H_2O$ and inoculated with an inoculum that had been cultivated at 50°C for 16 h.
103 The calculated cell density in the inoculated medium was 2.5–7.5 × 10^3 cells/ml. The glue was
104 applied to the adhesion surface of the Pyrex piece of the intermediate by using a toothpick. Next,
105 1.5 ml of inoculated medium were poured into the intermediate, followed by the adhesion of the

slide glass. The resultant product—an ATOC (Fig. 1b)—was left in the inverted position and weighed down using a disposable tube filled with 50 ml of water for at least 1 h. The ATOC was subsequently taken out of the workstation, and, for safety and easy handling, placed in a Petri dish in an inverted position. The ATOC in the Petri dish was incubated in a programmable incubator, with a temperature range from room temperature to 33°C for ≥10 h, then from 33°C to 68°C for 1 h 10 min, and finally, at 68°C for 7 h, which brought *T. globiformans* into the early stage of the mid-exponential phase. The ATOC was then observed using HTM. It should be noted that *T. globiformans* does not grow at the temperature range used in the first step of the incubation (Kuwabara et al. 2011).

Microscopic observations

HTM was performed using an upright optical microscope (Eclipse E600; Nikon, Tokyo, Japan) and a Microheat plate having a heating surface made of transparent glass (MP-10DMH; Kitazato Supply Co. Ltd., Shizuoka, Japan.), which had been modified by the manufacturer to electrically cancel the noise generated by periodic heating. An ATOC was attached to the Microheat plate with pieces of adhesive tape, and the entire apparatus was set on the movable stage of the microscope (Fig. 1c). A 40× objective was used to achieve a total magnification of 400×. Immersion oil was not used to avoid possible heat damage of the objective. When the Microheat plate was set at 80°C, the outer surface of the coverslip reached 65°C, as measured using a surface thermometer. The growing *T. globiformans* rods adhering to the inner surface of the coverslip were observed in the bright field without using phase contrast in order to obtain sufficient light intensity. Movies were taken using a

128 3CCD camera (HV-D28S; Hitachi Kokusai Electric, Tokyo, Japan), a video-capturing device (PC-
129 MDVD/U2; Buffalo, Nagoya, Japan), and a computer, and were processed using Premiere software
130 (version 6.5; Adobe Systems, San Jose, CA, USA).

131 Epifluorescence microscopy was performed using a LIVE/DEAD® *Bac*Light™ Bacterial
132 Viability Kit (hereafter, LIVE/DEAD; Molecular Probes, Eugene, OR, USA) or FM1-43 (Molecular
133 Probes). Images were captured using a CCD camera (ORCA-ER; Hamamatsu Photonics,
134 Hamamatsu, Japan) equipped with image acquisition and analysis software (AquaCosmos;
135 Hamamatsu Photonics) and a computer.

136 For field-emission scanning electron microscopy (FE-SEM), the cells were cultivated in Tc–S^0
137 medium with an SEM glass plate (diameter, 18 mm) in serum bottles. The glass plates on which
138 sessile rods grew were carefully taken out and fixed with 2% glutaraldehyde in 0.2 M sodium
139 cacodylate (pH 7.2) for 2 h at room temperature, and then processed as described previously
140 (Yoshida et al. 2006), except that post-fixation with osmium tetroxide was omitted. Briefly, fixed
141 samples were then dehydrated through a graded ethanol series (50%, 75%, 90%, 95%, and 100%)
142 by incubation for 15 min in each concentration, followed by substitution with dehydrated *t*-butyl
143 alcohol. The specimens were freeze-dried with a freeze drier VFD-21S (VACUUM DEVICE INC.,
144 Mito, Japan). The glass plates were mounted on specimen stubs. These specimens were coated with
145 platinum/palladium alloy with an ion-sputter E102 (Hitachi, Tokyo, Japan), and observed by field-
146 emission scanning electron microscope, JSM-6330F (JEOL, Akishima, Japan). For preparation of
147 free rods, the above culture was centrifuged at 1670 × *g* for 1 min to sediment aggregated cells and
148 debris. The supernatant was filtered through Nuclepore filters (pore size, 0.2 μm; Whatman, Clifton,
149 NJ, USA), and the filters were fixed in glutaraldehyde, dehydrated through the graded ethanol series,

and processed as described above.

For the thin sections, equal volumes of cell suspension in 2.0% (w/v) NaCl solution and a fixative solution containing 4% (w/v) glutaraldehyde in 0.2 M sodium cacodylate buffer (pH 7.2) were mixed (Kuwabara et al. 2011). After fixation at room temperature for 2 h, the cells were sedimented by centrifugation at 740 × *g* for 10 min. The sediments were washed with sodium cacodylate buffer and post-fixed with 1% osmium tetroxide in sodium cacodylate buffer at room temperature for 30 min. Fixed cells were sedimented using a hand-operated portable centrifuge, and the supernatant was discarded by decantation. The sediments were washed three times with sodium cacodylate buffer by hand-operated centrifugation and decantation. Sedimented cells were dehydrated through a graded ethanol series by keeping it in 30% and 50% ethanol for 45 min each, in 75%, 90%, and 95% ethanol for 15 min each, followed by 4 changes in 100% ethanol, each lasting for 15 min. The dehydrated pellet was first subjected to 2 changes of 10 min each of a 1:1 mixture of 100% ethanol and propylene oxide, and then to 2 changes of 10 min each of 100% propylene oxide. The propylene oxide was substituted with a 2:1, and then a 1:1 mixture of propylene oxide and Agar 100 Resin (Agar Scientific; Stansted, UK) for 30 min each. Then, cells were finally embedded in Agar 100 Resin. The resin containing cells was polymerized for 12 h at 70°C. Thin sections (40 nm) were cut using an ultramicrotome (EM-ULTRACUT·S; Reichert, New York, NY, USA) and double stained with drops of 2% (w/v) uranyl acetate for 20 min and lead citrate (Reynolds 1963) for 10 min; the stained sections were examined using a transmission electron microscope (TEM) (JEM1010; JEOL) operated at 80 kV.

Results

ATOC construction and usage

The initial stage of this study began with the use of the HTM system devised by Deguchi and Tsujii (2002) using a capillary cell; however, this method did not permit the observation of the periplasm. This may be because of the thick glass and curvature of the capillary impeding the achievement of the required resolution. Therefore, an ATOC using a coverslip with a regular thickness (0.17 mm) for optical microscopy observations was designed and manually constructed. It should be noted that the increase in the internal pressure could occur during growth due to water evaporation as well as due to the conversion of elemental sulfur to hydrogen sulfide and production of carbon dioxide as a result of bacterial metabolism; however, degassing of the medium could compensate for this increase in pressure.

HTM observation of cytokinesis and rod fission accompanied by abrupt sideward motion

In HTM, the periplasm was discerned between divided cells in growing rods, but not at the rod poles (Movie S1). Rods showing the intercellular periplasm eventually underwent fission at the middle of periplasm, indicating that rod fission occurs following cytokinesis and subsequent enlargement of the intercellular periplasm. The time between successive rod fission events was 38 ± 14 min (mean ± SD, n = 43) and the time from the recognition of the intercellular periplasm to the subsequent rod fission was 3.4 ± 1.8 min (n = 43). The interval between cytokinesis and rod fission

Movie S1

suggests that these 2 division events are achieved by different mechanisms in *T. globiformans*, whereas in *E. coli* they occur almost simultaneously by an FtsZ-dependent mechanism (Weiss 2004; Margolin 2005; Adams and Errington 2009). When rods fissioned, at least 1 of the newly generated rod poles abruptly moved sideward in all of the 43 rod fission events (for example, see Movie S1). Although electron microscopy with shadowing suggested that batch-cultured rods undergo fission by pulling apart (Kuwabara et al. 2011), no such motion has been observed in HTM, suggesting that solid-attached and free rods move differently upon fission.

Protrusions on sessile rods

Attachment of rods to solids may relate to the sideward motion upon rod fission. To elucidate the surface structures of glass-attached rods, the cells were cultivated in the presence of an SEM glass plate in a serum bottle and observed by FE-SEM. Sessile rods grown on the plate showed protrusions having a width of 120 ± 30 nm (n = 39), and their tips were either free or adhered to the plate (Fig. 2). Similar structures interconnecting the rods were also observed. However, free rods did not show any such protrusions. The abrupt sideward motion could relate to the glass-adhered protrusions, as discussed later. Protrusions were also observed by TEM (Fig. 3); they were found to be an expansion of the outer envelope and periplasm. Thus, these protrusions are considered to be nanotubes. The outer diameter of nanotubes was 100 ± 40 nm (n = 12), in the same range as the width of protrusions observed by FE-SEM.

Fig. 2

Fig. 3

Individual long cells contain nucleoids of different sizes

HTM observations showed that cells in newly fissioned rods were often considerably longer than average (for example, 6.9 μm as compared with the average of 3.5 μm (n = 86)). Examination of batch cultures confirmed the occurrence of long cells in the early stage of the mid-exponential phase, in which nucleoids were spread, with spaces between them, throughout the cytoplasm of individual cells (Fig. S1). Thus, the long cell production may not be an artifact of HTM. Close examination of batch-cultured long cells revealed that the nucleoids also have gaps within them, suggesting active DNA synthesis (Berlatzky et al. 2008) (Fig. 4a). In the middle stage of the mid-exponential phase, rods became shorter with nucleoids still spread throughout the cytoplasm (Fig. S1). From the late stage of the mid-exponential phase to the early stationary phase, the nucleoids occupied smaller regions in the cytoplasm. These findings suggest that the long cells having nucleoids of different sizes are generated only in the early stage of the mid-exponential phase. If the long cells in newly fissioned rods similarly have nucleoids of different sizes, it suggests that cell growth accompanying DNA synthesis is not tightly coupled with cytokinesis.

Fig. 4

Septal toga formation at rod fission sites

Formation of OM

Formation of septal OMs was studied using epifluorescence microscopy with FM1-43, which stains membranes. Many rods having 2 cells did not exhibit septal OMs or their FM1-43-stainable precursors in the intercellular periplasm (Fig. 4b, single asterisk). When the septal OMs were detected, they were necessarily situated at a distance from the cytoplasmic membranes and were already curved as a part of the daughter rods (Fig. 4b, double asterisk), suggesting that septal OMs

are formed after cytokinesis. Similarly, the cells occurring in chains, which were rare in single cultures but routinely observed in batch cultures (Kuwabara et al. 2011), did not show septal OMs or their FM1-43-stainable precursors in any intercellular periplasm (Fig. 4c). The mechanism of production of such multicellular rods is discussed later.

Formation of the amorphous layer

The next question is whether the amorphous layer is formed after the enlargement of the intercellular periplasm or almost simultaneously with cytokinesis as in *E. coli,* followed by the enlargement of the polar periplasms of daughter rods. TEM images showing the rod fission process were arranged to reflect its progression (Fig. 5). Cells appeared to divide by constriction, with a partially constricted outer envelope over the cell division site (Fig. 5a). Figure 5b shows a rare image, in which no discrete structure perpendicular to the rod axis was obvious in the intercellular periplasm. Most images showing the intercellular periplasm indicated a structure perpendicular to the rod axis at the constriction site of rods, which appeared to be continuous with the lateral gapped contour (Fig. 5c–f). The rod constriction site was not necessarily located at the center of the intercellular periplasm (Fig. 5d) and the septal amorphous layer was constructed on the structure perpendicular to the rod axis (Fig. 5e, f). Further constriction of the rod occurred when the septal amorphous layer became about twice as thick as the lateral one (Fig. 5g). Eventually, the daughter rods appeared to be pulled apart to undergo fission (Fig. 5h). These findings indicate that the septal amorphous layer is formed after the enlargement of intercellular periplasm, similar to the septal OM (Fig. 4b, double asterisk). The formation of both septal OM and amorphous layer in the intercellular

Fig. 5

periplasm suggests that the large periplasm serves to separate septal toga formation from cytokinesis.

Discussion

In the present study, the growth of *T. globiformans* attached to a coverslip was directly observed using HTM with an ATOC. If the rods did not produce protrusions, successive rod fission would not have been observed because the unattached rods were caused to flow away by the convection current in an ATOC (see Movie S1, 3 s after the start of movie, on the left side of the screen). Furthermore, dangling motion of rods suggests that they adhere to the coverslip via 1 point for each (Movie S2). Thus, adhesion to a coverslip appears to be essential for the observation of growth by HTM. Although poly-L-lysine is often used for the adhesion of microorganisms to glass, this technique did not work in HTM. Thus, natural adhesion may be necessary.

Movie S2

Sessile rods were found to have protrusions that adhered to the glass (Fig. 2). If these protrusions are protruded from moieties of a rod that are to be separated by fission (Fig. 2d), the newly generated rod poles will move sideward upon fission, escaping the growth of the other daughter rod. The abruptness of motion may be due to the release from the tension caused by growth of the daughter rods against one another. The natural motion of rods without adhesion to a solid would be to pull apart, as suggested by the shadowing of apparently just fissioned rods (Kuwabara et al. 2011), as well as by TEM image (Fig. 5h).

The protrusions of *T. globiformans* showed a width of 120 ± 30 nm on FE-SEM (Fig. 2) and of 100 ± 40 nm on TEM (Fig. 3). The difference in the averages may be due to the thickness of the

platinum/palladium alloy coating on FE-SEM. Recently, similar nanotubes having a width of 30–130 nm have been reported between sessile *Bacillus subtilis* cells, and suggested to be involved in intercellular communication (Dubey and Ben-Yehuda 2011). The authors also showed that similar structures were formed even between *B. subtilis* and *E. coli*, suggesting that nanotube formation occurs rather in general in sessile bacteria. Nanotube formation by *T. globiformans* would be the first finding of its type among thermophiles. Nanowires of *Shewanella oneidensis* strain MR-1 have a similar width (Gorby et al. 2006), although the presence of a tubular structure is unknown.

Epifluorescence microscopy with FM1-43 suggested that the septal OMs are formed in the intercellular periplasm in the last step of rod fission (Fig. 4b). This finding seems reasonable, as in *E. coli*, the septal OMs are formed in the last step of rod fission (Weiss 2004; Margolin 2005; Adams and Errington 2009). Because cytokinesis and septal toga formation do not occur simultaneously in *T. globiformans* (Fig. 5), cytokinesis could occur multiple times before septal toga formation, which may be the mechanism of the production of multicellular rods. Thus, the large periplasm is related to the multicellularity of *T. globiformans* (Kuwabara et al. 2011).

Acknowledgments

We thank Drs. Shigeru Deguchi and Sada-atsu Mukai of the Japan Agency for Marine-Earth Science and Technology for microscopic observations using their HTM system during the initial stages of this study, and Dr. Haruyo Yamaguchi for helping us with electron microscopy techniques. We are also grateful to Mr. Akitomo Kawasaki for some TEM work.

References

Adams DW, Errington J (2009) Bacterial cell division: assembly, maintenance and disassembly of the Z ring. Nat Rev Micro 7:642-653

Andrews KT, Patel BKC (1996) *Fervidobacterium gondwanense* sp. nov., a new thermophilic anaerobic bacterium isolated from nonvolcanically heated geothermal waters of the Great Artesian Basin of Australia. Int J Syst Bacteriol 46:265–269

Berlatzky IA, Rouvinski A, Ben-Yehuda S (2008) Spatial organization of a replicating bacterial chromosome. Proc Natl Acad Sci USA 105:14136-14140

Deguchi S, Tsujii K (2002) Flow cell for *in situ* optical microscopy in water at high temperatures and pressures up to supercritical state. Rev Sci Inst 73:3938–3941

Dubey GP, Ben-Yehuda S (2011) Intercellular nanotubes mediate bacterial communication. Cell 144:590-600

Gluch MF, Typke D, Baumeister W (1995) Motility and thermotactic responses of *Thermotoga maritima*. J Bacteriol 177:5473-5479

Gorby YA, Yanina S, McLean JS, Rosso KM, Moyles D, Dohnalkova A, Beveridge TJ, Chang IS, Kim BH, Kim KS, Culley DE, Reed SB, Romine MF, Saffarini DA, Hill EA, Shi L, Elias DA, Kennedy DW, Pinchuk G, Watanabe K, Ishii Si, Logan B, Nealson KH, Fredrickson JK (2006) Electrically conductive bacterial nanowires produced by *Shewanella oneidensis* strain MR-1 and other microorganisms. Proc Natl Acad Sci USA 103:11358-11363

Horn C, Paulmann B, Kerlen G, Junker N, Huber H (1999) In vivo observation of cell division of anaerobic hyperthermophiles by using a high-intensity dark-field microscope. J Bacteriol 181:5114–5118

Huber R, Langworthy TA, König H, Thomm M, Woese CR, Sleytr UB, Stetter KO (1986) *Thermotoga maritima* sp. nov. represents a new genus of unique extremely thermophilic eubacteria growing up to 90°C. Arch Microbiol 144:324–333

Huber R, Stetter KO (1992) The order Thermotogales. In: Balows, A, Trüper HG, Dworkin M, Harder W, Schleifer KH (eds) The Prokaryotes. Springer, New York, pp 3809–3815

Kuwabara T, Kawasaki A, Uda I, Sugai A (2011) *Thermosipho globiformans* sp. nov., an anaerobic thermophilic bacterium that transforms into multicellular spheroids with a defect in peptidoglycan formation. Int J Syst Evol Microbiol 61:1622-1627

Kuwabara T, Minaba M, Iwayama Y, Inouye I, Nakashima M, Marumo K, Maruyama A, Sugai A, Itoh T, Ishibashi J, Urabe T, Kamekura M (2005) *Thermococcus coalescens* sp. nov., a cell-fusing hyperthermophilic archaeon from Suiyo Seamount. Int J Syst Evol Microbiol 55:2507–2514

L'Haridon S, Miroshnichenko ML, Hippe H, Fardeau M-L, Bonch-Osmolovskaya E, Stackebrandt E, Jeanthon C (2001) *Thermosipho geolei* sp. nov., a thermophilic bacterium isolated from a continental petroleum reservoir in Western Siberia. Int J Syst Evol Microbiol 51:1327–1334

Margolin W (2005) FtsZ and the division of prokaryotic cells and organelles. Nat Rev Mol Cell Biol 6:862-871

Miranda-Tello E, Fardeau M-L, Thomas P, Ramirez F, Casalot L, Cayol J-L, Garcia J-L, Ollivier B (2004) *Petrotoga mexicana* sp. nov., a novel thermophilic, anaerobic and xylanolytic bacterium isolated from an oil-producing well in the Gulf of Mexico. Int J Syst Evol Microbiol 54:169–174

Weiss DS (2004) Bacterial cell division and the septal ring. Mol Microbiol 54:588-597

Wery N, Lesongeur F, Pignet P, Derennes V, Cambon-Bonavita M-A, Godfroy A, Barbier G (2001) *Marinitoga camini* gen. nov., sp. nov., a rod-shaped bacterium belonging to the order Thermotogales, isolated from a deep-sea hydrothermal vent. Int J Syst Evol Microbiol 51:495–504

Woese CR, Kandler O, Wheelis ML (1990) Towards a natural system of organisms: proposal for the domains Archaea, Bacteria, and Eucarya. Proc Natl Acad Sci USA 87:4576-4579

Yoshida M, Noël M-H, Nakayama T, Naganuma T, Inouye I (2006) A haptophyte bearing siliceous scales: ultrastructure and phylogenetic position of *Hyalolithus neolepis* gen. et sp. nov. (Prymnesiophyceae, Haptophyta). Protists 157:213-234

Figure legends

Fig. 1 **A**naerobic thermophile observation chamber (ATOC)

An intermediate construction of ATOC (a), a schematic illustration of completed ATOC (b), and an ATOC placed on a Microheat plate, which was set below an objective (c). CS, coverslip; M, medium; P, partition; PY, Pyrex piece; and SG, slide glass.

Fig. 2 FE-SEM images of sessile *Thermosipho globiformans* rods

Sessile rods adhered to aggregates of exopolysaccharide-like substance (asterisk) (a) and enlargement of the square showing protrusions (b). A protrusion from the proximal side of a rod to glass (c). A rod showing a future fission site (arrow) in between two glass-adhered protrusions (d). The width of the protrusions was 120 ± 30 nm (n = 39) when measured at the center of the length. Note that the large periplasm moieties at rod poles tended to be shrunken by dehydration during specimen preparation, and are not protrusions. Arrowheads, protrusions. Bars = 500 nm.

Fig. 3 TEM image of a *Thermosipho globiformans* rod having a protrusion

T. globiformans was batch-cultured to the mid-exponential phase in Tc–S^0 medium and analyzed by TEM. The square is enlarged in the inset. The width of the protrusions was 100 ± 40 nm (n = 12) when measured at the center of the length. It is notable that the envelope of protrusions was relatively densely stained. AL, amorphous layer. PP, periplasm. Bars = 500 nm and 100 nm (inset).

Fig. 4 Epifluorescence microscopy images of *Thermosipho globiformans* rods

Long cells in the early stage of the mid-exponential phase, as observed by phase-contrast

381 microscopy (a, upper panel), were observed by epifluorescence microscopy with LIVE/DEAD (a,
382 lower panel). Arrowheads, gaps in nucleoids. Arrows, spaces between nucleoids. Cells occurring in
383 pairs (b) and in a chain (c), as observed by phase-contrast microscopy (upper panels), were
384 observed by epifluorescence microscopy with FM1-43 (lower panels). A double asterisk shows the
385 polar OMs at the fission site of just-fissioning rods (b), while a single asterisk shows the absence of
386 polar OMs in the intercellular periplasms (b, c). Bars = 5 μm (a, b); 10 μm (c).
387
388 **Fig. 5** TEM images showing the process of rod fission of *Thermosipho globiformans*
389 Fission sites showing a dividing cell (a), no discrete structure in the periplasm between divided cells
390 (b), a structure perpendicular to the rod axis at a center (c) and a non-center (d) position in the
391 intercellular periplasm, a septal amorphous layer constructed on the perpendicular structure (e, f), a
392 nearly completed septal amorphous layer (g), and a septal amorphous layer extended to fission (h).
393 CM, cytoplasmic membrane. Arrows, structure perpendicular to the rod axis. Arrowheads, septal
394 amorphous layer. Bars = 100 nm.
395

Fig.1

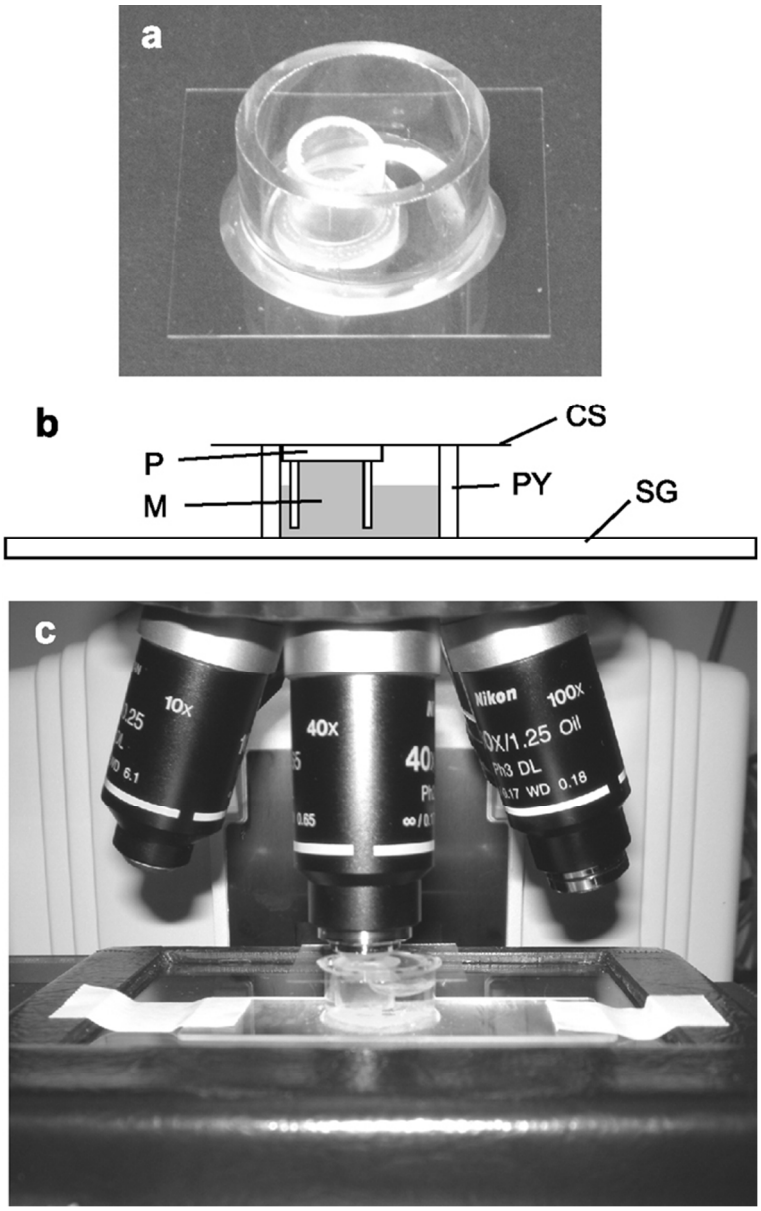

An intermediate construction of DOCUGAT (a), a schematic illustration of completed DOCUGAT (b), and a DOCUGAT placed on a Microheat plate, which was set below an objective (c). CS, coverslip; M, medium; P, partition; PY, Pyrex piece; and SG, slide glass.
60x95mm (300 x 300 DPI)

Fig.2

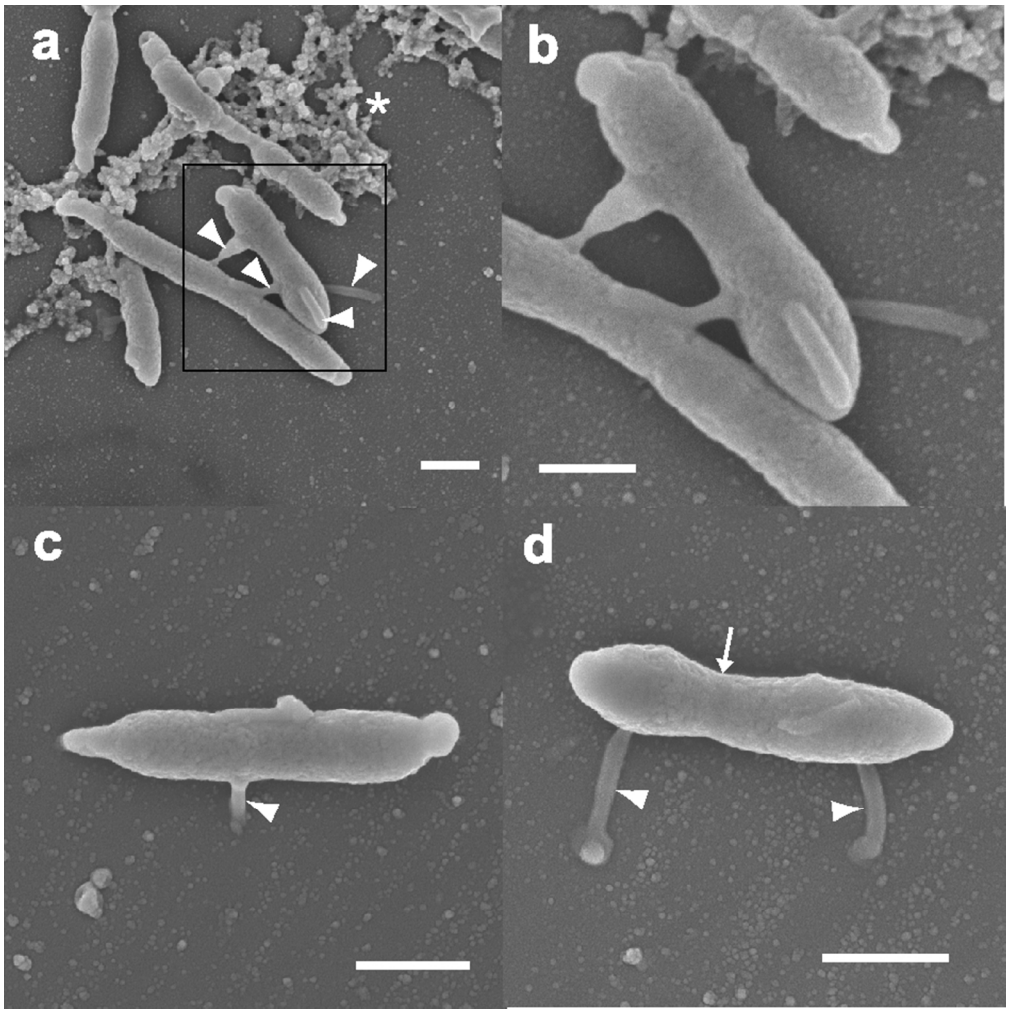

Sessile rods adhered to aggregates of exopolysaccharide-like substance (asterisk) (a) and enlargement of the square showing protrusions (b). A protrusion from the proximal side of a rod to glass (c). A rod showing a future fission site (arrow) in between two glass-adhered protrusions (d). The width of the protrusions was 140 (40) nm (n = 39) when measured at the center of the length. Note that the large periplasm moieties at rod poles tended to be shrunken by dehydration during specimen preparation, and are not protrusions. Arrowheads, protrusions. Bars = 500 nm.
79x79mm (300 x 300 DPI)

Fig.3

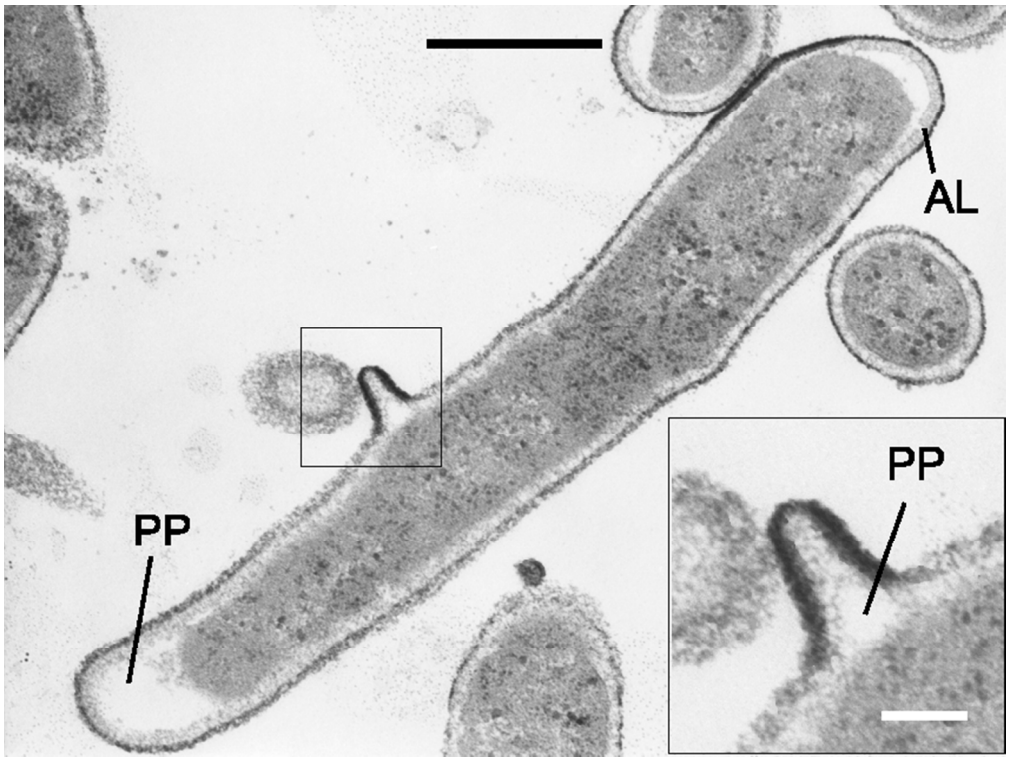

The square is enlarged in the inset. T. globiformans was batch-cultured to the mid-exponential phase in Tc–S0 medium. The width of the protrusions was 100 (40) nm (n = 12) when measured at the center of the length. It is notable that the envelope of protrusions was relatively densely stained. AL, amorphous layer. PP, periplasm. Bars = 500 nm and 100 nm (inset).
71x54mm (300 x 300 DPI)

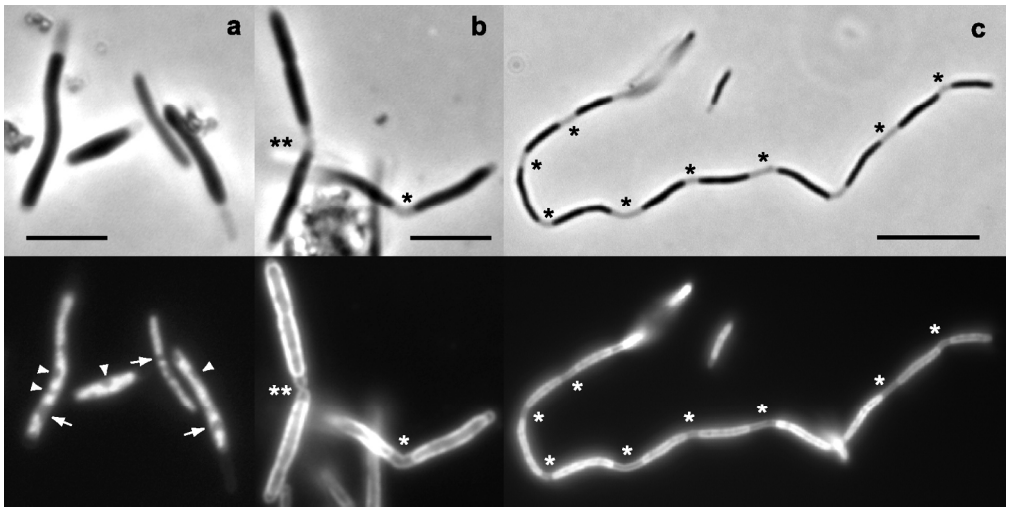

Long cells in the early stage of the mid-exponential phase, as observed by phase-contrast microscopy (a, upper panel), were observed by epifluorescence microscopy with LIVE/DEAD (a, lower panel). Arrowheads, gaps in nucleoids. Arrows, spaces between nucleoids. Cells occurring in pairs (b) and in a chain (c), as observed by phase-contrast microscopy (upper panels), were observed by epifluorescence microscopy with FM1-43 (lower panels). A double asterisk shows the polar OMs at the fission site of just-fissioning rods (b), while a single asterisk shows the absence of polar OMs in the intercellular periplasms (b, c). Bars = 5 μm (a, b); 10 μm (c).
159x79mm (300 x 300 DPI)

Fig.5

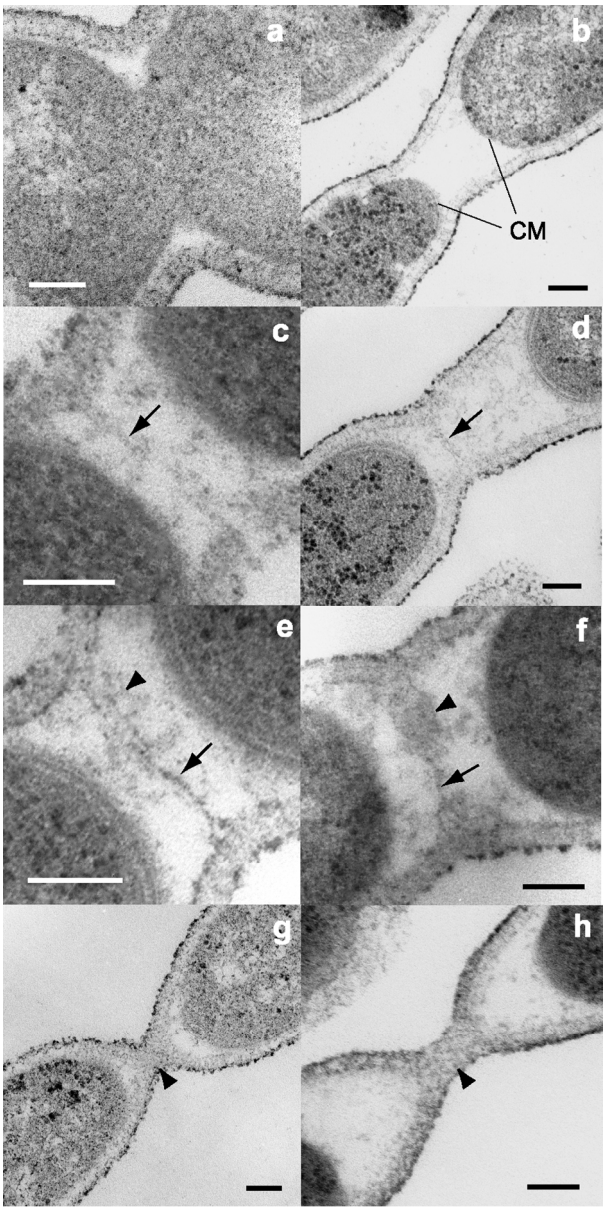

Fission sites showing a dividing cell (a), no discrete structure in the periplasm between divided cells (b), a structure perpendicular to the rod axis at a center (c) and a non-center (d) position in the intercellular periplasm, a septal amorphous layer constructed on the perpendicular structure (e, f), a nearly completed septal amorphous layer (g), and a septal amorphous layer extended to fission (h). CM, cytoplasmic membrane. Arrows, structure perpendicular to the rod axis. Arrowheads, septal amorphous layer. Bars = 100 nm.
79x159mm (300 x 300 DPI)